The International Journal of Advanced Manufacturing Technology (2019) 103:1175–1184
https://doi.org/10.1007/s00170-019-03617-1

ORIGINAL ARTICLE

The cooling rate dependence of the specific volume in amorphous plastic injection molding

Kristjan Krebelj[1] · Miroslav Halilovič[1] · Nikolaj Mole[1]

Received: 13 February 2019 / Accepted: 18 March 2019 / Published online: 2 April 2019
© Springer-Verlag London Ltd., part of Springer Nature 2019

Abstract
In numerical simulation of injection molding, the specific volume is important for the cavity pressure prediction, which governs the part properties, such as shrinkage and warpage. The specific volume is often considered as a function of pressure and temperature only. This neglects its cooling rate dependence. The related degradation of the cavity pressure prediction usually remains unknown. In this work, the cooling rate effect is modeled and the discrepancy is quantified for amorphous polystyrene. A rate equation is used to model the specific volume relaxation within the scope of three-dimensional computational fluid dynamics. The model incorporates the mold compliance to allow a comparison to the experimental results. The cavity pressure evolution and the final residual stresses are calculated for both the modeled and the neglected cooling rate effects. This provides argumentation for either neglecting or modeling the phenomenon.

Keywords Injection molding · Numerical simulation · Specific volume relaxation · Amorphous polymer · Residual stresses

1 Introduction

1.1 Motivation

During injection molding, the cavity pressure governs the following important part properties: residual stresses, shrinkage, and warpage. However, accurate predictions of the cavity pressure evolution are challenging, because it is the result of multiple phenomena, some of which are difficult to predict, e.g., mold compliance [1, 2] and mold contact thermal resistance [3, 4]. Additionally, the specific volume of the material depends on the cooling rate [5, 6]. By increasing the cooling rate, the glass transition in amorphous polymers shifts towards higher temperatures. The cooling rate in a 1-mm-thick cavity is generally two or three orders of magnitude greater than during the material characterization procedure which renders the specific volume data less accurate. This work investigates the impact of the phenomenon by developing a computational fluid dynamics (CFD) model. The model incorporates a description of the cooling rate dependence of the specific volume and quantifies its importance on the prediction of the cavity pressure evolution.

1.2 Literature overview

This literature overview discusses the general contributions to the numerical simulation of injection molding and the contributions to the modeling of the cooling rate-dependent specific volume which are relevant to this work.

Numerical injection molding simulation has advanced with numerous scientific and commercial contributions, which was thoroughly described by Kennedy and Zheng [7]. Much of the research was performed in the scope of the residual stress prediction. Baaijens [8], for instance, developed a model, capable of describing the filling and packing stages as well as the final residual stresses. The model demonstrated the importance of mold compliance for the prediction of the cavity pressure evolution. The modeling was extended with various contributions, by advancing the constitutive modeling [9], geometry description [10], and residual stress calculation [11]; the residual stress prediction contributions were reviewed by Guevara-Morales and Figueroa-López [12].

✉ Nikolaj Mole
nikolaj.mole@fs.uni-lj.si

Kristjan Krebelj
kristjan.krebelj@fs.uni-lj.si

Miroslav Halilovič
miroslav.halilovic@fs.uni-lj.si

[1] Faculty of Mechanical Engineering, University of Ljubljana, Aškerčeva 6, 1000 Ljubljana, Slovenia

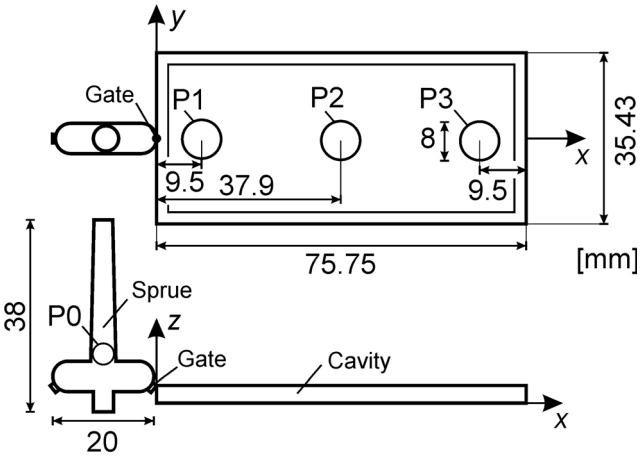

Fig. 1 Mold cavity geometry

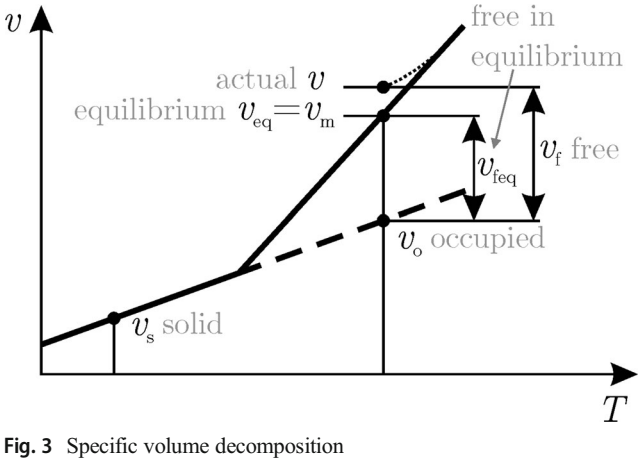

Fig. 3 Specific volume decomposition

The simulations were typically formulated describing the specific volume according to the Tait equation of state. This makes the glass transition a function of temperature and pressure only, while it generally also depends on the cooling rate [13]. The glass transition was explained as a visco-elastic phenomenon by Ferry [5]. Knauss and Emri [6] modeled the time evolution of the specific volume with respect to a transient thermo-mechanical excitation and demonstrated an agreement of the results with the experimental data. The cooling rate dependence of the glass transition is, thus, explained as a lagging volume relaxation.

Some contributions to the numerical modeling of injection molding have considered the volume relaxation effect. Yu et al. [14, 15] modeled the development of the residual stresses and the final density distribution in injection molding of a thin wall. Ghoneim and Hieber [16] employed a fully viscoelastic approach to model the solidification of a thin wall. Zheng et al. [17] have formulated an injection molding model, but the cooling rate effect was only considered for the semi-crystalline polymers. Lee and Kwon [18] included the cooling rate-dependent volumetric behavior of an amorphous polymer in a simulation of injection molding. According to the concept of free volume [5], they described the volumetric behavior using a differential equation resembling the Maxwell rheological model. The equation had already been used by Yu and Kalyon [15] who had demonstrated its equivalence to the fictive temperature approach [19]. The time-dependent specific volume modeling is adopted in this work in a variation which is detailed later on. Notable contributions were also made by Kabanemi et al. [20, 21] and Zhou et al. [22], who formulated injection molding models where the bulk modulus was time-dependent but had not investigated its significance.

1.3 Scope

The relevant contributions in the literature have employed thin-wall assumptions, i.e., geometrical simplifications within the model. These are dismissed in this work allowing the modeling to be performed on non-simplified three-dimensional geometry. The current approach makes no use of infinitesimal strain theory and formulates the free volume relaxation based on the Tait equation making it suitable for the implementation within the CFD modeling. This is because in the scope of the CFD, the material volumetric behavior is more

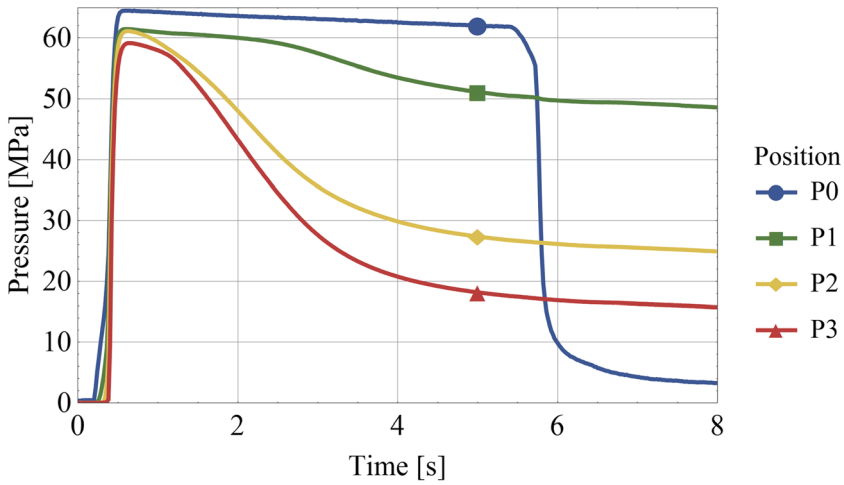

Fig. 2 Measured cavity pressure evolutions

accurately described by an equation of state than by individual material constants, i.e., moduli and thermal expansion coefficients. The model incorporates the following three influences on the cavity pressure evolution: mold compliance, pressure-dependent thermal contact with the mold, and the cooling rate-dependent specific volume. This allows comparing the prediction to the experimental pressure evolution.

2 Methodology

The goal of this paper is to determine the significance of volume relaxation in the prediction of the cavity pressure in the injection molding. This is done by comparing the simulated results for the following both cases:

- the case with the volume relaxation accounted for; and
- the case that ignores the volume relaxation.

The difference in the calculated pressure is due to the presence of the volume relaxation. The result may be used as a reference when considering the importance of the phenomenon in injection molding simulation.

The approach to developing the comparison is achieved through the following steps:

- formulate a description of the volume relaxation in amorphous plastics;
- include the description in a CFD model;
- validate the model with experiments from the literature and injection molding pressure measurements; and
- assess the effect of volume relaxation on the cavity pressure.

This section first describes the experimental investigation, introducing the material of interest and the measured pressure evolutions which are later used in the experimental validation. The volumetric material model is then described and included in CFD to model the actual injection molding process.

Table 1 Tait equation parameters from [23]

	Melt	Solid	Unit
b_1	$9.72 \cdot 10^{-4}$	$9.72 \cdot 10^{-4}$	m^3/kg
b_2	$6.044 \cdot 10^{-7}$	$2.248 \cdot 10^{-7}$	$m^3/(kgK)$
b_3	$1.85 \cdot 10^{8}$	$2.64 \cdot 10^{8}$	Pa
b_4	$4.93 \cdot 10^{-3}$	$3.51 \cdot 10^{-3}$	K^{-1}
b_5	377.23		K
b_6	$0.3495 \cdot 10^{-7}$		K/Pa

2.1 Experimental investigation

Injection molding experiments were conducted on a Boy 50M injection molding machine with the maximum clamping force of 500 kN. The injection rate during filling was set to 10 cm^3/s, yielding a filling time of approximately 0.3 s. The packing pressure was set to 63 MPa. The mold was tempered with water of 50 °C, and the melt temperature was set to 230 °C. The injected material was polystyrene Styron PS 678E. According to Vietri et al. [23], the number average molecular weight of the material is $M_n = 87$ kg/mol and the weight average $M_w = 250$ kg/mol. This is an amorphous thermoplastic which was often used in research and is, thus, well-described in the literature [2, 24, 25]. The mold cavity is schematically depicted in Fig. 1. The cavity pressure evolution was measured during the injection molding of plaques. The pressure measurement positions are denoted by P0 to P3.

The measurements of pressure were performed using measuring pins installed in the mold, behind which a force sensor of type Z1342/10000 (producer Hasco GmbH) was positioned. Their signal was captured by an amplifier of type Z134, also produced by Hasco GmbH, outputting a 0 to 10 V analog voltage signal. The signal was sampled at 100 Hz with the resolution of 1.22 mV yielding a resolution of 0.03 MPa in the pressure measurement. Based on the calibration procedure, an error of ± 1% is estimated. The measured cavity pressure evolutions are reported in Fig. 2. Further details and results from the particular experimental procedure are reported in [26].

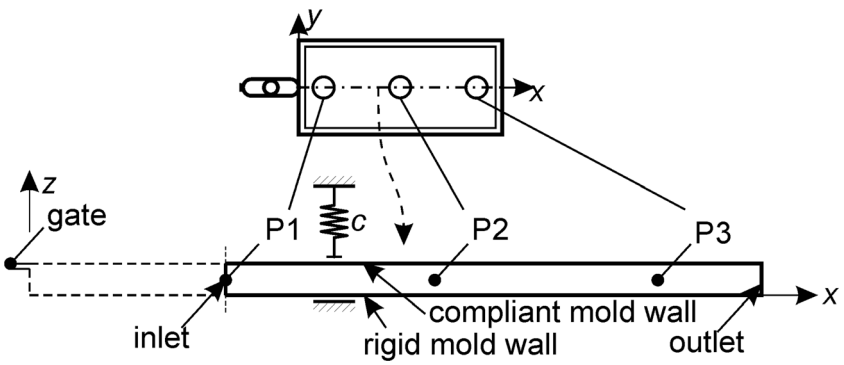

Fig. 4 Computational domain

Table 2 Cross-WLF viscosity model parameters [23]

	Melt	Unit
n	0.252	1
τ	30.8	kPa
D_1	47.6	GPa/s
D_2	373.15	K
D_3	0.51[a]	K/MPa
A_1	25.7	1
A_2	61.06	K

[a] Substituted

2.2 Specific volume description

The specific volume for the injection molding simulation was in the literature often described by the Tait equation of state, e.g., by Baaijens [8] as a volumetric constitutive model and by Ghoneim and Hieber [16], to calculate the compressibility and the thermal expansion to formulate a viscoelastic constitutive description. In this section, the Tait equation of state is directly incorporated into the free volume relaxation differential equation, which was used by Yu and Kalyon [15] and Lee and Kwon [18].

2.2.1 Specific volume decomposition

According to the Tait equation for amorphous polymers, the melt specific volume is expressed as a function of pressure p and temperature T:

$$v_m = (b_{1m} + b_{2m}(T - b_5))\left(1 - C\ln\left(1 + \frac{p}{b_{3m}\exp(-b_{4m}(T - b_5))}\right)\right); \quad (1)$$

for $T > T_{tr}$, and the solid specific volume:

$$v_s = (b_{1s} + b_{2s}(T - b_5))\left(1 - C\ln\left(1 + \frac{p}{b_{3s}\exp(-b_{4s}(T - b_5))}\right)\right); \quad (2)$$

for $T \le T_{tr}$, where $T_{tr} = b_5 + b_6 p$.

The subscripts "m" and "s" denote the b parameters' values for the melt and solid domains, respectively, with the universal constant $C = 0.0894$.

According to Ferry [5], the (specific) volume, v, of an amorphous polymer can be described as the sum of the occupied volume, v_o, and the free volume, v_f:

$$v = v_o + v_f, \quad (3)$$

as shown in Fig. 3.

The volume of the solid is the occupied volume, v_o, plus the non-relaxed free volume, v_f, due to quenching. The latter is here neglected by assuming sufficiently slow cooling during the measurement. The Tait equation expression of the solid, v_s, is then used as an approximation of the sole occupied volume, $v_o = v_s$. By extrapolation, as described by Ferry [5], $v_o = v_s$ can be assumed within the fluid domain. The expression for v_m is then used to compute the total equilibrium volume $v_{eq} = v_m$ of the melt. Following Eq. (3), the equilibrium free volume, v_{feq}, is calculated as the difference of the Tait equation expressions of the melt and solid domains

$$v_{feq} = v_{eq} - v_o = v_m - v_s. \quad (4)$$

Analogously to the approach of Lee and Kwon [18], a rate equation with a relaxation time, τ_r, is used to describe the actual free volume, v_f, i.e., its transition to its equilibrium value, v_{feq}:

$$\frac{dv_f}{dt} = -\frac{v_f - v_{feq}}{\tau_r}, \quad (5)$$

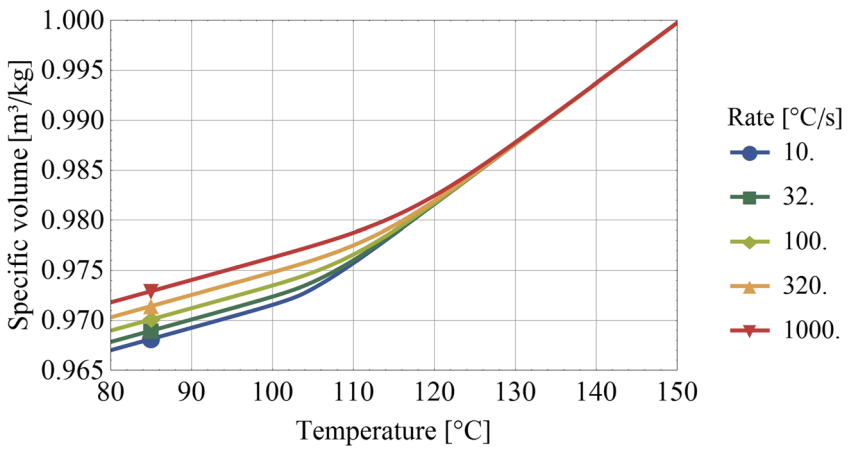

Fig. 5 Glass transition for relevant cooling rates

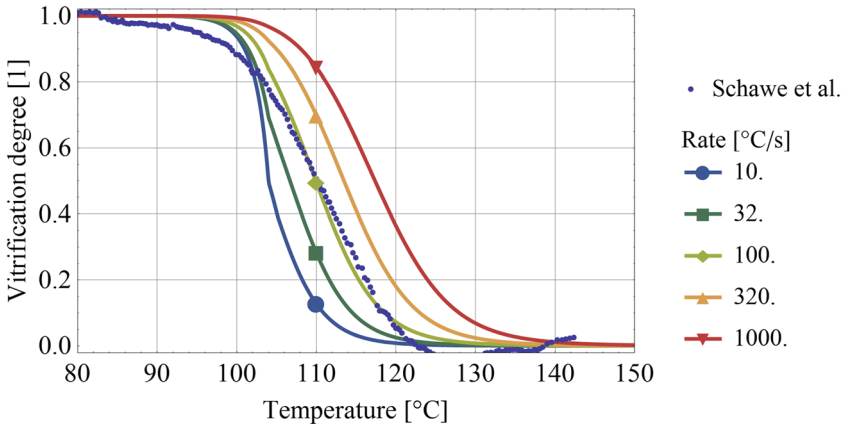

Fig. 6 Vitrification degree

with the initial condition $v_f = v_{feq}$. The total specific volume is finally given as

$$v = v_s + v_f. \tag{6}$$

2.2.2 Relaxation time

The volumetric relaxation depends on temperature and pressure. It slows down with cooling and pressurization and eventually leads to vitrification, i.e., the glass transition of the material [5, 6]. Within the scope of the numerical simulation of injection molding, a convenient description of the change in the relaxation time, τ_r, is the WLF equation [27] because it is part of the frequently used Cross-WLF melt viscosity model:

$$\eta_0(T,p) = D_1 \exp\left(-\frac{A_1(T-D_2-D_3p)}{A_2+T-D_2}\right) \tag{7}$$

$$\eta(\dot{\gamma},T,p) = \frac{\eta_0(T,p)}{1+\left(\frac{\eta_0(T,p)\dot{\gamma}}{\tau^*}\right)^{n-1}} \tag{8}$$

where p is pressure, T temperature, $\dot{\gamma}$ generalized shear rate, and the rest are material parameters. A common assumption states that all time-dependent phenomena are governed by the lagging molecular reconfiguration [5]. Following the time–temperature–pressure superposition principle [6], the relaxation time, τ_r, is expressed as the product of the reference relaxation time, τ_{ref}, scaled by a shift factor, a_T:

$$\tau_r = \tau_{ref} a_T \tag{9}$$

where the shift factor can be assumed to follow the WLF equation [5, 27]:

$$a_T = \exp\left(-\frac{A_1(T-D_2-D_3p)}{A_2+T-D_2}\right). \tag{10}$$

2.3 Injection molding model formulation

The modeling of the specific volume was tested with a model of the injection molding filling and packing stages. The code employs the finite volume method to solve the differential conservation equations for the mass, momentum, and energy. It was developed by modifying the *compressibleInterFoam* solver from OpenFOAM 3.0.1 [28]. It solves the problem of a laminar, non-isothermal, compressible flow of two immiscible fluids according to the volume of fluid method. The model is presented from the constitutive and the geometrical aspect.

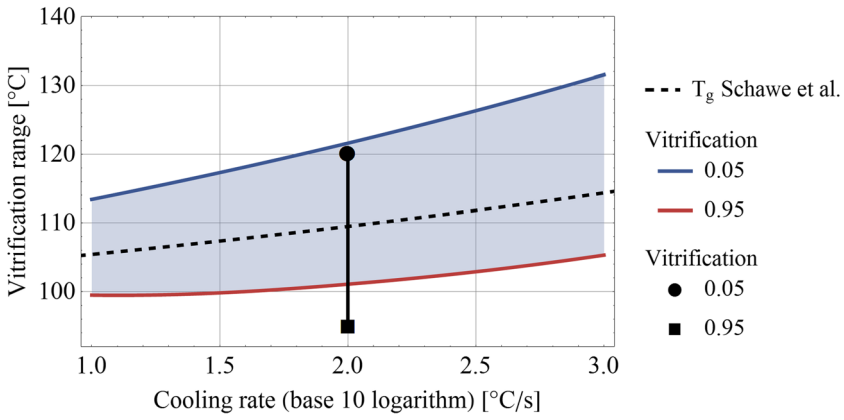

Fig. 7 Glass transition for the relevant cooling rates

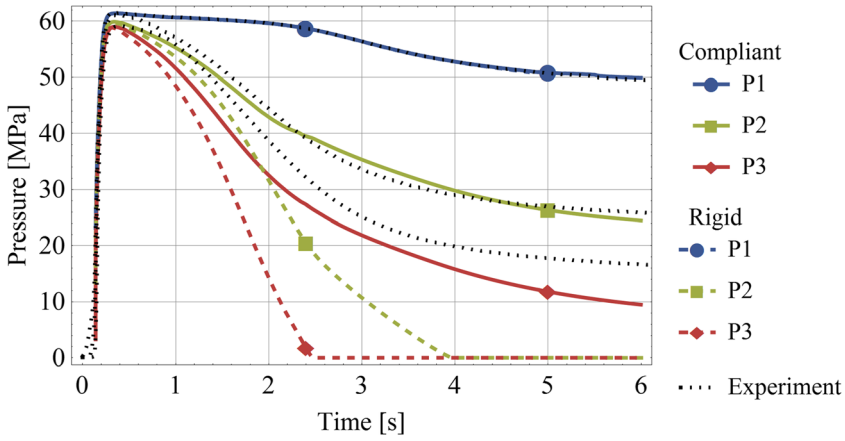

Fig. 8 Cavity pressure evolution during packing

2.3.1 Constitutive modeling

The stresses, σ_{ij}, are composed of the hydrostatic pressure, p, the elastic contribution, τ^{e}_{ij}, in the solidified material, and the viscous contribution, τ^{v}_{ij}, as

$$\sigma_{ij} = -p\,\delta_{ij} + \tau^{e}_{ij} + \tau^{v}_{ij}, \tag{11}$$

with the Kronecker delta tensor, δ_{ij}, using Einstein's notation with $i, j = 1, 2, 3$. The viscosity and specific volume were modeled as described in the previous section, and the viscous deviatoric stress was calculated as:

$$\tau^{v}_{ij} = 2\,\eta\,D^{d}_{ij}, \tag{12}$$

where D^{d}_{ij} is the deviatoric component of the rate of deformation tensor. The melt was assumed to solidify when reaching the maximum viscosity of 5 MPas, at which point, the deviatoric elasticity was onset according to the Upper Convected Maxwell model [22] with an infinite relaxation time:

$$\frac{\partial \tau^{e}_{ij}}{\partial t} + u_k \frac{\partial \tau^{e}_{ij}}{\partial x_k} - \frac{\partial u_i}{\partial x_k}\tau^{e}_{kj} - \frac{\partial u_j}{\partial x_k}\tau^{e}_{ik} = 2GD^{d}_{ij} \tag{13}$$

where τ^{e}_{ij} is the elastic deviatoric stress, u_i is the velocity vector, x_i are the Cartesian coordinates, $G = 907$ MPa is the shear modulus [29], and D^{d}_{ij} is the deviatoric rate of deformation tensor. The thermal conductivity was adopted from Dawson et al. [30], and the specific heat from Jansen et al. [24] as done in [26].

2.3.2 Geometry and boundary conditions

The cavity was described by the longitudinal cross-section displayed in Fig. 4. The measured P1 pressure was used as the boundary condition. This eliminated the gate from the computational domain where the flow is not planar. The air was released through the outlet during the filling stage, whereas, during the packing stage, the outlet was closed.

The melt filling temperature was 230 °C, and the mold temperature 50 °C. The heat transfer coefficient, h, on the mold walls was modeled as pressure-dependent with a linear interpolation between the points $(p, h) = (0$ MPa, 1020 W/(m^{2}K)) and (100 MPa, 5384 W/(m^{2}K)) as identified from the work of Delaunay et al. [4]. The compliance of the cavity was set to $c = 0.75$ μm/MPa. The value for the particular mold was first heuristically determined in [26] as 0.5 μm/MPa, but

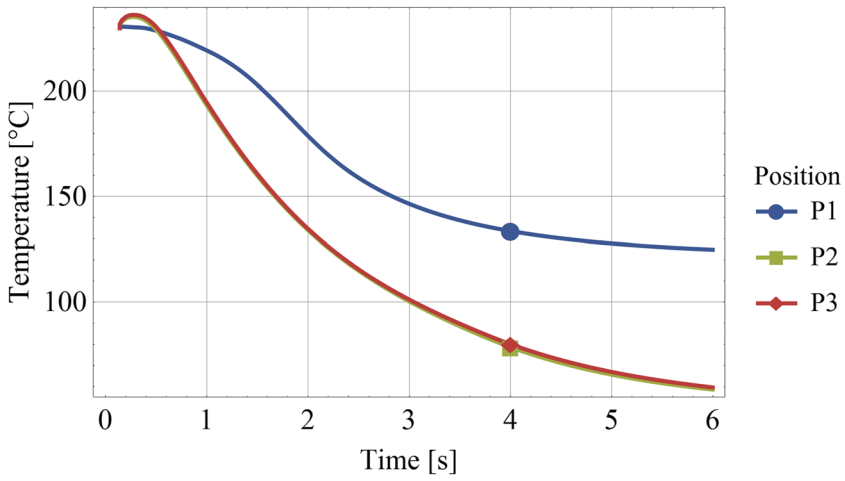

Fig. 9 Temperature evolutions at the P1, P2, and P3 positions

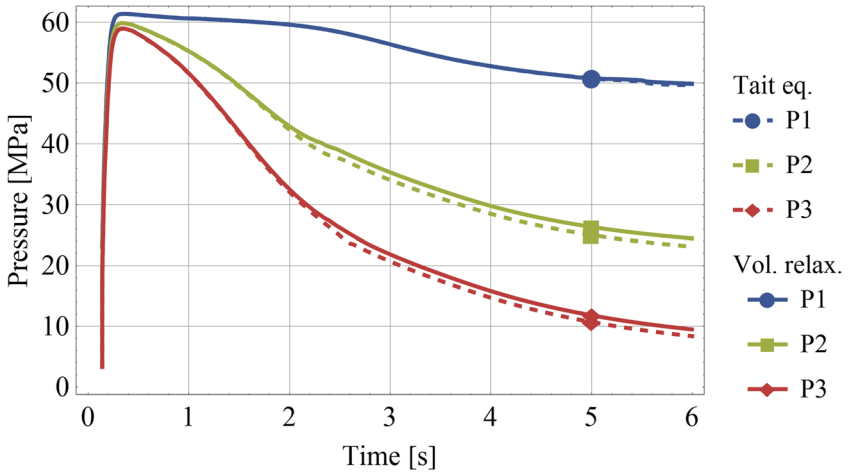

Fig. 10 Comparison of the computed cavity pressure evolution for the modeled and ignored volumetric relaxation

it was, in this work, increased, since the current model also describes the actual material flow. The appropriateness of the choice is confirmed later on in the experimental validation by inspecting the result obtained with a rigid cavity. The finite volume mesh consisted of 32 cells in the thickness direction and 1200 cells in the length direction.

2.3.3 Material parameters

The Tait equation parameters for PS Styron 678E are adopted from Vietri et al. [23] who report the values from the Moldflow® material database (Table 1).

The Cross-WLF parameters are adopted from the Moldflow® material database as reported by Vietri et al. [23] (Table 2). In Eq. (10), the D_3 parameter is set to b_6 from the Tait equation to match its pressure shift in temperature and with 0 in Eq. (7), because pressure dependence of viscosity was not significant in the performed experiments [26].

The reference relaxation time, τ_{ref}, was related to the results of high cooling rate experiments. For the case of the polystyrene used in the experimental part of this work, $\tau_{ref} = 2$ s is heuristically deduced from fast scanning calorimetry testing from the literature; a similar polystyrene was studied by Schawe [13] (BASF, PS168N, $M_n = 95$ kg/mol and $M_w = 270$ kg/mol). See Fig. 5 for the cooling rate-dependent specific volume according to Eq. (6).

3 Experimental validation

3.1 Specific volume modeling

The glass transition is a continuous process. In this work, it was quantified by a vitrification degree, r, ranging from 0 to 1, as a linear transformation of c_p or dv/dT. Figure 6 depicts values of the vitrification degree corresponding to the curves in Fig. 5, together with the vitrification degree of a specific heat measurement from Schawe [31] at a cooling rate of 100 K/s. This supports the choice of $\tau_{ref} = 2$ s for the particular cooling rate. Vitrification progress for other cooling rates is confirmed as reasonable in Fig. 7.

The vitrification span is obtained from Fig. 6 for the r values between 0.05 and 0.95 and plotted in Fig. 7. The glass

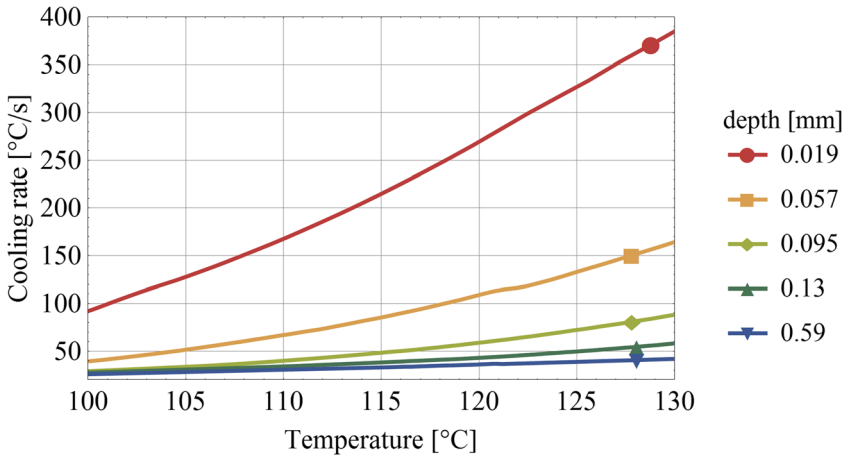

Fig. 11 Cooling rate in the solidification temperature range

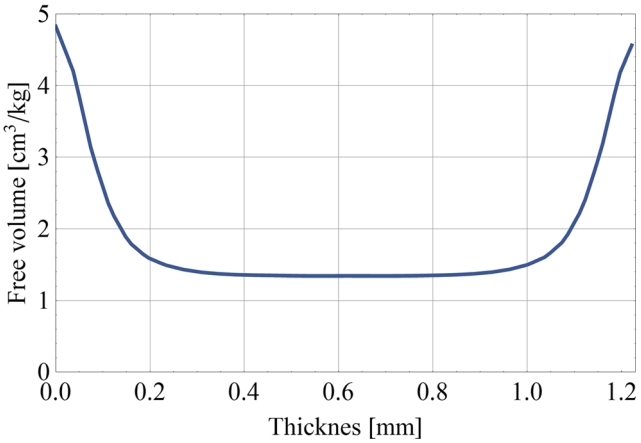

Fig. 12 Free volume along the thickness

transition temperature according to Schawe [13] is shown in Fig. 7 to fall well within the glass transition temperature range of Eq. (6) with the heuristically determined $\tau_{ref} = 2$ s. Based on Fig. 7, the modeling of the cooling rate effect on the specific volume is judged appropriate.

3.2 Injection molding simulation

The pressure evolution during packing is presented in Fig. 8. The P1 pressure matched the measurement, because it was imposed on the boundary, but the computed P2 and P3 pressure evolutions were used to assess the validity of the solution. The computed pressure decay was found to reproduce the measured accelerated drop in the first 2 s due to the rapid viscosity increase, while in the final 4 s the pressure change slowed down due to temperature stabilization. A quantitative agreement of practical value was found between the experimental and computed results. Comparison of the compliant-mold solution to the rigid-mold solution supports the choice of the mold compliance.

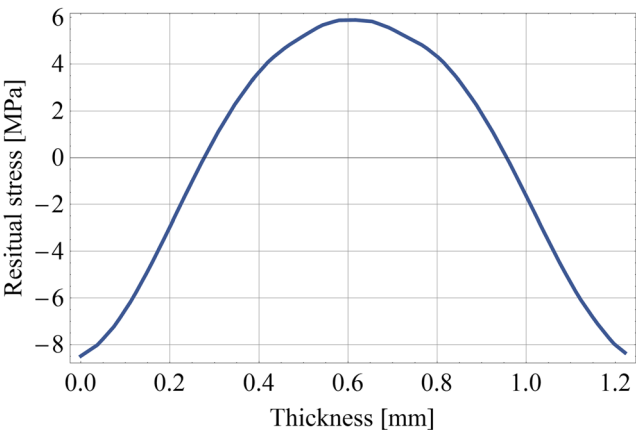

Fig. 13 Residual stress distribution in the thickness direction

4 Results and discussion

The temperature and the pressure results are informative about the process and are presented in the following. The cooling rates are also examined because of their influence on the glass transition. Lastly, the residual stresses are shown because they govern part quality and have been examined in the literature both numerically and experimentally.

The temperature evolution at the three positions of interest is depicted in Fig. 9. At the start of the compression, a temperature rise was predicted on the positions P2 and P3 due to the thermodynamic–mechanical coupling. At these two positions, the temperature evolutions were practically identical, because the cavity is rather short. The results at the position P1 were probed at the center of the boundary cell and were influenced by the solution field in addition to the boundary condition.

The key result of this work is reported in Fig. 10. The calculated cavity pressure is compared for two cases. The primary result includes the modeled volume relaxation, while the secondary result, depicted with the dashed lines, only models the specific volume according to the Tait equation of state. Virtually, no difference was predicted for the first 1.2 s when the cavity is occupied by a predominantly molten material. During this first interval, the cavity pressure was governed by the viscous behavior which established the pressure gradient. With the onset of solidification, the addition of material was reduced and the volumetric behavior gained prominence. The inclusion of volume relaxation implied approximately 1 MPa higher cavity pressure in the cooling phase.

Analyzing the temperature evolution in the cavity center and near the mold surface allows predicting the relevant cooling rates. The cooling rate was plotted against the temperature in Fig. 11 for the temperature range of possible solidification. For the cavity center, the cooling rate at solidification was predicted to be around 30 K/s whereas the surface cooled within the 100 to 400 K/s.

The distribution of free volume through the thickness at the P2 position is displayed in Fig. 12 at time $t = 6$ s. With the specific volume of solid polystyrene around 1000 cm^3/kg, the additional free volume ranged between 0.1 and 0.5% of the total specific volume. In accordance with the cooling rate analysis from Fig. 11, the material beneath the depth of 0.2 mm retained a nearly constant free volume of 1.4 cm^3/kg.

The final residual stress, σ_x, in the thickness distribution is shown in Fig. 13. The tensile core is enclosed by compressive layers as computed and measured in the literature [29] for plaques from the same material but in different conditions. The order of magnitude of the computed residual stresses also agrees with the results from the literature [29]. The tensile surface stress that has often been reported in the literature [29, 32, 33] is not developed here, because it would require pronounced surface layer solidification at low pressure [32].

Depending on the simulation's purpose, the effect of volume relaxation may be judged either significant or insignificant. The variation in cavity pressure was of the order of experimental error, which could support the argumentation of neglecting volume relaxation in simulation of conventional injection molding. On the other hand, a significant variation of free volume was predicted in the surface layers in Fig. 12, which offers insight into the impact of rapid surface cooling. This supports the approach of accounting for the volume relaxation in the simulation of precision injection molding of lenses, where the density variation can affect diffraction of light and alter the optical properties [34].

5 Conclusion

The volumetric behavior for amorphous thermoplastics was described by a differential equation, which is suitable for implementation in the CFD software and allows for capturing the effect of the cooling rate on the glass transition temperature. Basing the modeling on the Tait equation of state and the WLF equation was particularly convenient because of their frequent use in injection molding simulation and the readily available material parameters.

The shift in the glass transition temperature was demonstrated to have mildly influenced the cavity pressure evolution, but the material state through the thickness was found to vary. Quantitative argumentation was provided to judge the importance of modeling the phenomenon of volumetric relaxation.

Two suggestions for future work can be considered at this point. A possible extension would be to employ viscoelastic relaxation of the deviatoric stresses. This would allow a more precise prediction of the material inflow and, therefore, a closer approximation of the pressure decay. The other advancement possibility would also be to perform measurements of the residual stresses and assess the validity of the prediction.

Acknowledgements This research did not receive any specific grant from funding agencies in the public, commercial, or not-for-profit sectors.

References

1. Delaunay D, Le Bot P, Fulchiron R et al (2000) Nature of contact between polymer and mold in injection molding. Part II: influence of mold deflection on pressure history and shrinkage. Polym Eng Sci 40:1692–1700. https://doi.org/10.1002/pen.11301
2. Pantani R, Speranza V, Titomanlio G (2001) Relevance of mold-induced thermal boundary conditions and cavity deformation in the simulation of injection molding. Polym Eng Sci 41:2022–2035
3. Bendada A, Derdouri A, Lamontagne M, Simard Y (2004) Analysis of thermal contact resistance between polymer and mold in injection molding. Appl Therm Eng 24:2029–2040. https://doi.org/10.1016/j.applthermaleng.2003.12.027
4. Delaunay D, Le Bot P, Fulchiron R et al (2000) Nature of contact between polymer and mold in injection molding. Part I: influence of a non-perfect thermal contact. Polym Eng Sci 40:1682–1691. https://doi.org/10.1002/pen.11300
5. Ferry JD (1980) Viscoelastic properties of polymers. John Wiley & Sons, Inc
6. Knauss WG, Emri I (1987) Volume change and the nonlinearly thermo-viscoelastic constitution of polymers. Polym Eng Sci 27:86–100. https://doi.org/10.1002/pen.760270113
7. Kennedy P, Zheng R (2013) Flow analysis of injection molds. Hanser Publishers, Cincinnati
8. Baaijens FPT (1991) Calculation of residual stresses in injection molded products. Rheol Acta 30:284–299. https://doi.org/10.1007/BF00366642
9. Chang R-Y, Chiou S-Y (1995) A unified K-BKZ model for residual stress analysis of injection molded three-dimensional thin shapes. Polym Eng Sci 35:1733–1747
10. Chang R, Yang W (2001) Numerical simulation of mold filling in injection molding using a three-dimensional finite volume approach. Int J Numer Methods Fluids 37:125–148
11. Kamal MR, Lai-Fook RA, Hernandez-Aguilar JR (2002) Residual thermal stresses in injection moldings of thermoplastics: a theoretical and experimental study. Polym Eng Sci 42:1098–1114
12. Guevara-Morales A, Figueroa-López U (2014) Residual stresses in injection molded products. J Mater Sci 49:4399–4415. https://doi.org/10.1007/s10853-014-8170-y
13. Schawe JEK (2015) Measurement of the thermal glass transition of polystyrene in a cooling rate range of more than six decades. Thermochim Acta 603:128–134. https://doi.org/10.1016/j.tca.2014.05.025
14. Yu JS, Wagner AH, Kalyon DM (1992) Simulation of microstructure development in injection molding of engineering plastics. J Appl Polym Sci 44:477–489
15. Yu JS, Kalyon DM (1991) Development of density distributions in injection molded amorphous engineering plastics. Part II. Polym Eng Sci 31:153–160. https://doi.org/10.1002/pen.760310303
16. Ghoneim H, Hieber CA (1997) Incorporation of density relaxation in the analysis of residual stresses in molded parts. Polym Eng Sci 37:219–227
17. Zheng R, Kennedy P, Phan-Thien N, Fan X-J (1999) Thermoviscoelastic simulation of thermally and pressure-induced stresses in injection moulding for the prediction of shrinkage and warpage for fibre-reinforced thermoplastics. J Non-Newton Fluid Mech 84:159–190. https://doi.org/10.1016/S0377-0257(98)00148-7
18. Lee YB, Kwon TH (2001) Modeling and numerical simulation of residual stresses and birefringence in injection molded center-gated disks. J Mater Process Technol 111:214–218
19. Tool AQ (1946) Relation between inelastic deformability and thermal expansion of glass in its annealing range. J Am Ceram Soc 29:240–253. https://doi.org/10.1111/j.1151-2916.1946.tb11592.x
20. Kabanemi KK, Aït-Kadi A, Tanguy PA (1995) Prediction of residual flow and thermoviscoelastic stresses in injection molding. Rheol Acta 34:97–108
21. Kabanemi KK, Vaillancourt H, Wang H, Salloum G (1998) Residual stresses, shrinkage, and warpage of complex injection molded products: numerical simulation and experimental validation. Polym Eng Sci 38:21–37. https://doi.org/10.1002/pen.10162
22. Zhou H, Xi G, Liu F (2008) Residual stress simulation of injection molding. J Mater Eng Perform 17:422–427. https://doi.org/10.1007/s11665-007-9156-6
23. Vietri U, Sorrentino A, Speranza V, Pantani R (2011) Improving the predictions of injection molding simulation software. Polym Eng Sci 51:2542–2551. https://doi.org/10.1002/pen.22035

24. Jansen KMB, van Dijk DJ, Burgers EV (1998) Experimental validation of shrinkage predictions for injection molded products. Int Polym Process 13:99–104. https://doi.org/10.3139/217.980099
25. Jansen KMB, Pantani R, Titomanlio G (1998) As-molded shrinkage measurements on polystyrene injection molded products. Polym Eng Sci 38:254–264. https://doi.org/10.1002/pen.10186
26. Krebelj K, Mole N, Štok B (2017) Three-dimensional modeling of the stress evolution in injection molded parts based on a known melt pressure field. Int J Adv Manuf Technol 90:2363–2376. https://doi.org/10.1007/s00170-016-9533-0
27. Williams ML, Landel RF, Ferry JD (1955) The temperature dependence of relaxation mechanisms in amorphous polymers and other glass-forming liquids. J Am Chem Soc 77:3701–3707. https://doi.org/10.1021/ja01619a008
28. Weller HG, Tabor G, Jasak H, Fureby C (1998) A tensorial approach to computational continuum mechanics using object-oriented techniques. Comput Phys 12:620. https://doi.org/10.1063/1.168744
29. Zoetelief WF, Douven LFA, Housz AJI (1996) Residual thermal stresses in injection molded products. Polym Eng Sci 36:1886–1896. https://doi.org/10.1002/pen.10585
30. Dawson A, Rides M, Nottay J (2006) The effect of pressure on the thermal conductivity of polymer melts. Polym Test 25:268–275. https://doi.org/10.1016/j.polymertesting.2005.10.001
31. Schawe JEK (2014) Vitrification in a wide cooling rate range: the relations between cooling rate, relaxation time, transition width, and fragility. J Chem Phys 141:184905. https://doi.org/10.1063/1.4900961
32. Jansen K (1994) Residual stresses in quenched and injection moulded products. Int Polym Process 9:82–89
33. Bushko WC, Stokes VK (1995) Solidification of thermoviscoelastic melts. Part I: formulation of model problem. Polym Eng Sci 35:351–364. https://doi.org/10.1002/pen.760350409
34. Greener J (2006) Precision injection molding: process, materials, and applications. Hanser

Publisher's note Springer Nature remains neutral with regard to jurisdictional claims in published maps and institutional affiliations.